Measurement of Arterial Activity on Routine FDG PET/CT Images Improves Prediction of Risk of Future CV Events

Amparo L. Figueroa, MD, MPH,* Amr Abdelbaky, MD,* Quynh A. Truong, MD, MPH,*† Erin Corsini, BS,* Megan H. MacNabb, BA,* Zachary R. Lavender, BA,* Meredith A. Lawler, BA,* Steven K. Grinspoon, MD,‡ Thomas J. Brady, MD,* Khurram Nasir, MD, MPH,§‖ Udo Hoffmann, MD, MPH,* Ahmed Tawakol, MD*†

Boston, Massachusetts; Miami, Florida; and Baltimore, Maryland

OBJECTIVES   This study sought to determine whether arterial inflammation measured by ^{18}F-fluoro-deoxyglucose positron emission tomography (^{18}F-FDG-PET) improves prediction of cardiovascular disease (CVD) beyond traditional risk factors.

BACKGROUND   It is unknown whether arterial ^{18}F-FDG uptake measured with routine PET imaging provides incremental value for predicting CVD events beyond Framingham risk score (FRS).

METHODS   We consecutively identified 513 individuals from 6,088 patients who underwent ^{18}F-FDG-PET and computed tomography (CT) imaging at Massachusetts General Hospital between 2005 and 2008 and who met additional inclusion criteria: ≥30 years of age, no prior CVD, and free of cancer. CVD events were independently adjudicated, while blinded to clinical data, using medical records to determine incident stroke, transient ischemic attack, acute coronary syndrome, revascularization, new-onset angina, peripheral arterial disease, heart failure, or CVD death. FDG uptake was measured in the ascending aorta (as target-to-background-ratio [TBR]), while blinded to clinical data.

RESULTS   During follow-up (median 4.2 years), 44 participants developed CVD (2 per 100 person-years at risk). TBR strongly predicted subsequent CVD independent of traditional risk factors (hazard ratio: 4.71; 95% confidence interval [CI]: 1.98 to 11.2; p < 0.001) and (hazard ratio: 4.13; 95% CI: 1.59 to 10.76; p = 0.004) after further adjustment for coronary calcium score. Addition of arterial PET measurement to FRS scores improved the C-statistic (mean ± standard error 0.62 ± 0.03 vs. 0.66 ± 0.03). Further, incorporation of TBR into a model with FRS variables resulted in an integrated discrimination of 5% (95% CI: 0.36 to 9.87). Net reclassification improvements were 27.48% (95% CI: 16.27 to 39.92) and 22.3% (95% CI: 11.54 to 35.42) for the 10% and 6% intermediate-risk cut points, respectively. Moreover, TBR was inversely associated with the timing of CVD (beta −0.096; p < 0.0001).

CONCLUSIONS   Arterial FDG uptake, measured from routinely obtained PET/CT images, substantially improved incident CVD prediction beyond FRS among individuals undergoing cancer surveillance and provided information on the potential timing of such events.   (J Am Coll Cardiol Img 2013;6:1250–9) © 2013 by the American College of Cardiology Foundation

Tools such as the Framingham risk score (FRS) are widely used to assess risk of cardiovascular disease (CVD) and provide a basis for the determination of optimal primary prevention strategies (1,2). However, the majority of CV events occur in individuals who are stratified as having low to intermediate risk by such risk assessment tools (3–5). Accordingly, better risk assessment tools are needed. Although the added benefit of blood biomarkers has been documented over the years, no more than modest improvements over traditional risk factors for predicting CV events have been observed (3,5–7), thus prompting interest in the use of imaging biomarkers.

^{18}F-fluorodeoxyglucose positron emission tomography (^{18}F-FDG-PET), an imaging modality that is routinely used for cancer surveillance, allows quantification of ^{18}F-2-deoxy-D-glucose uptake within the artery wall (a correlate of atherosclerotic inflammation), which has emerged as a marker of atherosclerosis (8,9). Although studies show evidence of an association between increased arterial FDG uptake and vascular events observed in a population of individuals with active cancer (10,11), no prior study has directly evaluated its incremental predictive value over traditional risk factors and none has evaluated the utility of the signal on cancer-free patients not currently receiving cancer chemotherapy. Accordingly, we evaluated the incremental utility of arterial FDG uptake, measured using PET/computed tomography (CT) for predicting incident CVD. To do so, we identified cancer-free patients undergoing routine PET/CT scans for cancer surveillance and tested the hypothesis that the FDG-PET signal improves prediction of incident CV events.

METHODS

Study population. Study participants (N = 513) were consecutively identified from a database of 6,088 patients who had undergone ^{18}F-FDG-PET and CT imaging for oncological evaluation at the Massachusetts General Hospital between 2005 through 2008. Pre-defined inclusion criteria were: 1) absence of prior cancer diagnosis or remission from cancer at the time of PET imaging and throughout the follow-up period; 2) ≥30 years of age; 3) no prior history of CVD; and 4) absence of acute or chronic inflammatory or autoimmune disease (based on documented medical history) or use of chronic anti-inflammatory therapy. Participants were required to have at least 3 clinical visit notes (spanning ≥1 year) to ensure that sufficient clinical data were available (including that of the FRS for 10-year CVD risk components such as age [years], sex, systolic blood pressure [mm Hg], current smoking [within 1 year], diabetes, total cholesterol [mg/dl], and high-density lipoprotein cholesterol [mg/dl]) (12) to determine clinical status around the time of PET imaging. PET and CT images were collected for blinded analysis, and clinical data were routed for blinded event adjudication by an adjudication committee (Fig. 1). The study protocol was approved by the local human research committee.

Outcome events. CVD was herein defined according to the manner used to determine FRS risk categories (12): incident ischemic stroke or transient ischemic attack, acute coronary syndrome, revascularization (coronary, carotid, or peripheral), new-onset angina, peripheral arterial disease (PAD), heart failure, or CVD death. Events were clinically adjudicated by 2 cardiologists using clinically available records (Online Appendix).
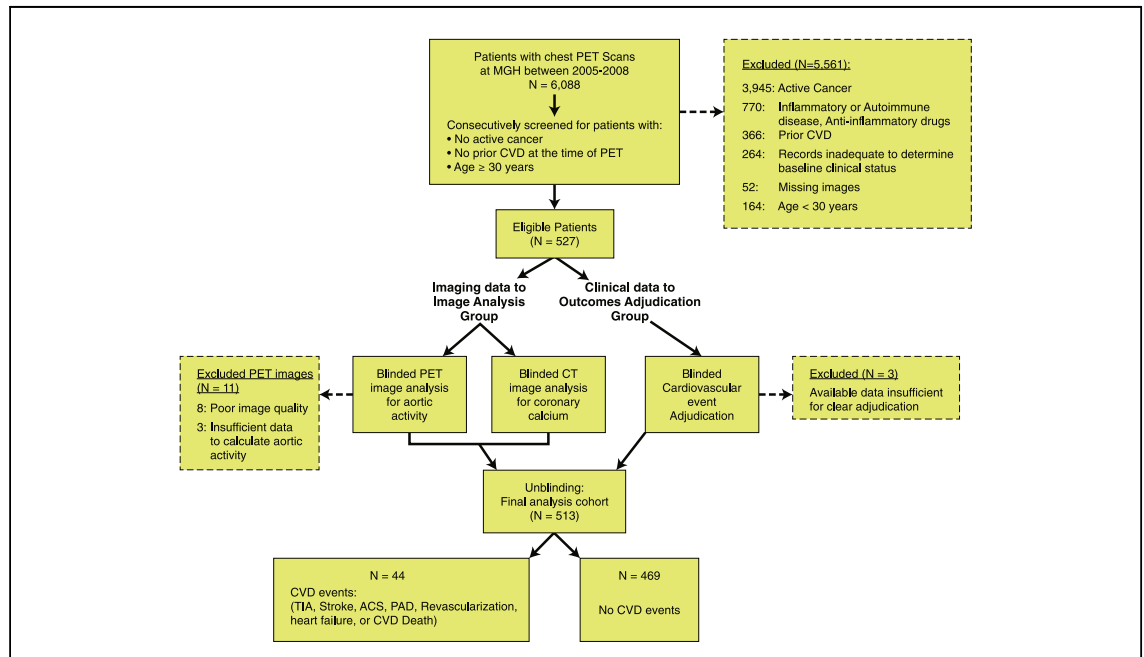
PET/CT protocol and image analysis. Whole-body FDG-PET imaging was performed per clinical protocol using a Biograph 64 (Siemens, Forchheim, Germany) or similar system. FDG was administered at approximately 370 MBq (10 mCi) intravenously after an overnight fast. PET images were acquired in 3-dimensional mode approximately 60 min later. Patients were imaged in the supine position, and images were obtained over 15 to 20 min. Low-dose, nongated, non–contrast-enhanced CT

ABBREVIATIONS AND ACRONYMS

CAC = coronary artery calcium

CT = computed tomography

CVD = cardiovascular disease

^{18}F-FDG-PET = ^{18}F-fluorodeoxyglucose positron emission tomography

FRS = Framingham risk score

hs-CRP = high-sensitivity C-reactive protein

NRI = net reclassification index

PAD = peripheral arterial disease

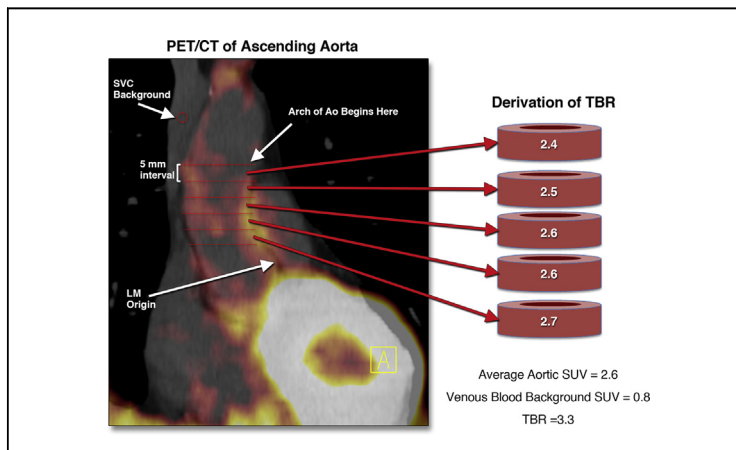**SUV** = standardized uptake value

TBR = target-to-background ratio

Figure 1. Schematic Diagram of Patient Selection

Analysis cohort was derived from a database of patients who underwent whole-body ^{18}F-fluorodeoxyglucose positron emission tomography (^{18}F-FDG-PET) scans for clinical indications. The ^{18}F-FDG-PET imaging at the time the participants met inclusion and exclusion criteria serve as the start of follow-up. All exclusions were made prior to unblinding of imaging data. Missing images represent patients who were eligible but had missing PET or computed tomography (CT) images. Available data insufficient for clear adjudication represent patients who experienced other events that did not meet adjudication criteria for cardiovascular disease (CVD) (2 patients excluded because events could not be clearly adjudicated based on available clinical data and 1 patient excluded due to development of right carotid dissection during follow-up, which neither qualified for incident CVD or no CVD). ACS = acute coronary syndrome; MGH = Massachusetts General Hospital; PAD = peripheral arterial disease; TIA = transient ischemic attack.

Figure 2. FDG Uptake Measurement

FDG uptake was evaluated within the wall of the aorta on axial images. At each axial section, a region of interest (ROI) was drawn around the wall of the aorta and the maximum standardized FDG uptake value (SUV$_{max}$) was recorded. The thickness of each axial slice was approximately 5 mm. Subsequently, the target-to-background ratio (TBR) was calculated by dividing the mean of all axial slice SUV$_{max}$ (approximately 6 to 8 slices per patient) by the venous blood SUV$_{max}$ obtained from the superior vena cava (average of 10 ROIs) to correct for the blood compartment contribution. Ao = aorta; LM = left main artery; SVC = superior vena cava; other abbreviations as in Figure 1.

(120 keV, 50 mAs) was used for attenuation correction prior to the PET scan.

FDG uptake measurement. PET-CT images were batch-analyzed by an investigator blinded to the patients' clinical information according to previously described methods (13). FDG uptake was evaluated within the wall of the ascending aorta and superior vena cava (as maximum and mean standardized FDG uptake value [SUV$_{max}$ and SUV$_{mean}$, respectively]) approximately every 5 mm on axial images, a location with excellent reproducible measures of FDG uptake (14). Subsequently, the target-to-background ratio (TBR) was reported (ratio of the average arterial to blood axial slice SUV$_{max}$) to correct for the blood compartment contribution (15). TBR is a reproducible method (14,15) for measuring arterial FDG uptake that has been shown to correlate with histological markers of inflammation (Fig. 2) (9,16) and has been used in a majority of other studies (17–19).

Coronary artery calcium score assessment. Coronary artery calcium (CAC) score was evaluated by a separate group of investigators (E.C. and U.H.) than those who performed the PET/CT analyses

using standardized methods (20) while blinded to clinical information and PET data. Details are provided in the Online Appendix.

Statistical analysis. Descriptive data are presented as mean ± SD for continuous parametric variables, median (interquartile range [IQR]) for continuous nonparametric data, and frequency with proportions for nominal variables, as appropriate. The Fisher exact test was used to evaluate differences in proportions. For comparison of continuous variables, Student t test was used for parametric and Mann-Whitney U test for nonparametric data. Kaplan-Meier estimates of CVD-free events of patients stratified by tertiles of FDG uptake expressed as TBR or SUV were calculated. We prospectively sought to threshold TBR data based on data distribution. We subsequently thresholded TBR data into tertiles for 2 reasons: 1) tertiles have a better model fit compared with a median cut point; and 2) tertiles will not reduce statistical power significantly compared with using more than 3 thresholds. Cox proportional hazards regression was used to calculate hazard ratios and 95% confidence interval. Additionally, the incremental value of TBR beyond the FRS components was assessed by the following methods: 1) concordance probability estimate, a C-statistic for data with censoring (21); and 2) net reclassification improvement (NRI) applied to survival data (22). The association between TBR and the timing of CVD was also evaluated using a linear regression analysis with TBR as the outcome and timing of CVD as ordinal predictor. Further, we modeled CAC score using 3 categories (0 to 10, 11 to 99, and ≥100) (23). See the Online Appendix for details on CAC assessment. All analyses were performed using SAS 9.2 (Cary, North Carolina). A 2-sided p value <0.05 was considered statistically significant. Additional details regarding the statistical analysis is provided in the Online Appendix.

RESULTS

Baseline characteristics of the entire cohort and subgroups are shown in Table 1 and Online Tables S1 and S2. Distribution of risk factors including TBR and CAC was similar between the full cohort and the subgroup with complete FRS variables. Overall, 44 participants developed CVD (rate 2 per 100 person-years at risk) in 6.5 years (median 4.2 years; range 0.02 to 6.55). Major CV events (acute myocardial infarction, ischemic stroke, and arterial revascularization) were observed at a rate of 1.49 per 100 person-years of follow-up. In the

subgroup of cancer survivors or patients with previous history of cancer (n = 429), 28 developed CVD (rate 1.65 per 100 person-years at risk). Among the cancer-naive population (n = 84), 16 developed CVD (rate 5 per 100 person-years at risk). The median follow-up period was 4.2 years (range 0.02 to 6.55 years, measured from the participants' index FDG-PET imaging to their latest clinical follow-up or electronic medical record on file as of May 8, 2012, or development of any CVD).

CV events. CV events were adjudicated as follows: 21 acute coronary syndrome events (17 acute myocardial infarctions and 4 unstable angina), 17 coronary revascularizations, 2 ischemic strokes, 2 transient ischemic attacks, 7 nonischemic strokes, 1 carotid revascularization, 6 new-onset angina (1 with and 5 without occlusive disease documented on invasive coronary angiogram), 4 new diagnosis of PAD, 2 peripheral revascularizations secondary to PAD, and 2 subsequent CV deaths due to acute myocardial infarction. Additionally, 4 subsequent non-CV deaths were registered during the follow-up period.

Cox regression. For the entire cohort, participants in the highest TBR tertile (≥2.2) had an increased risk for CVD compared with individuals in the lowest TBR tertile (≤1.84): 4.71 (IQR: 1.98 to 11.2; p = 0.0004), after adjustment for age and CV risk factors (Fig. 3). After further adjustment for CAC score, the association remained robust with a hazard ratio of 4.13 (IQR: 1.59 to 10.76; p = 0.004). Similar observations were made when CVD outcomes were restricted to major CV events (adjusted CVD risk was higher in patients in the highest TBR tertile compared with the lowest tertile: 2.95 [IQR: 1.08 to 8.06; p = 0.035]). With the uncorrected arterial PET measurement (i.e., the aortic SUV$_{max}$ without dividing by venous background SUV$_{max}$), similar data were yielded: an increased adjusted CVD risk was observed in patients in the highest tertile (≥2.29) versus lowest tertile (≤1.83), 2.67 (IQR: 1.02 to 6.97; p = 0.04) (Online Table S3).

As anticipated, CAC measured on nongated CT scans was observed to be predictive of CVD. CAC scores of 11 to 99 and ≥100 were associated with a 3.45- (IQR: 1.56 to 7.6; p = 0.002) and 3.02- (1.29 to 7.05; p = 0.01) fold higher CVD risk compared with CAC scores of ≤10. Moreover, individuals with higher TBR remained at greater risk for CVD after adjustment for FRS variables and CAC score (5.76; IQR: 1.79 to 18.57; p = 0.0003).

The FDG-PET/CT signal provided prognostic information in both cancer survivors as well as cancer-naive individuals. An intertertile increase in TBR was associated with an increased adjusted

Table 1. Baseline Characteristics

	Full Cohort (N = 513)	Participants Without Subsequent CVD (n = 469)	Subjects With Subsequent CVD (n = 44)	p Value
Age, yrs	55 (45–66)	54 (44–65)	67 (61–78)	<0.001
Male	215 (42)	196 (42)	19 (43)	0.87
Current smoker	55 (11)	42 (9)	13 (30)	<0.001
Body mass index, kg/m^2*	27 (23–31)	26 (23–31)	27 (25–31)	0.26
Hypertension	181 (35)	155 (33)	26 (59)	<0.001
Hyperlipidemia	143 (28)	125 (27)	18 (41)	0.05
Diabetes	46 (9)	38 (8)	8 (18)	0.046
Statin users	103 (20)	86 (18)	17 (39)	0.003
Antihypertensive therapy	182 (35)	154 (33)	28 (64)	<0.001
FDG uptake (TBR)	2.0 (0.28)	1.96 (1.79–2.15)	2.19 (1.94–2.32)	<0.001
Systolic blood pressure*	123 ± 15	123 ± 15	126 ± 13	0.16
Lipid profile*				
Total cholesterol	192 ± 43	193 ± 44	186 ± 39	0.40
Triglycerides	109 (79–156)	100 (73–150)	130 (86–175)	0.05
High-density lipoprotein	57 ± 18	58 ± 18	50 ± 14	0.005
Low-density lipoprotein	111 ± 37	111 ± 38	109 ± 33	0.70
FRS, 10-yr % risk of general CVD*	9.6 (4.75–18.25)	9 (4–17)	18.8 (10.65–27.45)	<0.001
ATP III 10-yr risk categories, %				
<10	134 (51.54)	125 (56.8)	9 (22.5)	<0.001
10–20	71 (27.31)	58 (26.4)	13 (32.5)	
>20	55 (21.15)	37 (16.8)	18 (45)	
<6	77 (29.62)	74 (33.6)	3 (7.5)	<0.001
6–20	128 (49.23)	109 (49.6)	19 (47.5)	
>20	55 (21.15)	37 (16.8)	18 (45)	
CAC score*	0 (0–15.89)	0 (0–6.36)	19.13 (0–82)	<0.0001
0–10	329 (73.44)	313 (75.6)	16 (47.06)	
11–99	61 (13.62)	51 (12.32)	10 (29.41)	
≥100	58 (12.95)	50 (12.08)	8 (23.53)	0.0001
Race				
White	464 (90.45)	424 (90.4)	40 (90.91)	
Black or African American	17 (3.31)	16 (3.4)	1 (2.27)	
Asian	14 (2.73)	12 (2.6)	2 (4.55)	0.86
Hispanic	17 (3.31)	16 (3.4)	1 (2.27)	
American Indian	1 (0.19)	1 (0.21)	0	

Continued on the next page

(for age and risk factors, including CAC) CVD risk in both cancer-naïve individuals (4.26; IQR: 1.60 to 11.32; p = 0.004) as well as cancer survivors (2.06; IQR: 1.12 to 3.78; p = 0.02). For the subgroup analyses, no effect modifications by previous cancer therapies were observed (Online Table S4).

Association between FDG uptake and timing of CVD. Arterial PET signals provide information regarding the potential timing of subsequent CVD

events. Individuals with the highest TBRs were more likely to experience near-term CVD. The mean TBR (SD) in each of the groups of individuals who developed CVD at 0 to 6 months, 7 to 24 months, and >24 to 79 months and no events in 79 months were 2.27 (0.34), 2.16 (0.29), 2.12 (0.23), and 1.98 (0.28), respectively (Fig. 4). Arterial inflammation (TBR) was inversely related to the timing of CVD (beta −0.096; p < 0.0001).

Table 1. Continued

|	Full Cohort (N = 513)	Participants Without Subsequent CVD (n = 469)	Subjects With Subsequent CVD (n = 44)	p Value
Prior history of cancer	429 (83.63)	401 (86)	28 (64)	
Cancer type				
None	84 (16.37)	68 (14.5)	16 (36.36)	
Lymphoma	189 (36.84)	182 (38.8)	7 (15.91)	
Gynecologic	83 (16.18)	79 (16.8)	4 (9.09)	<0.001
Gastrointestinal	49 (9.55)	43 (9.2)	6 (13.64)	
Lung	20 (3.9)	16 (3.4)	4 (9.09)	
Head and neck	38 (7.41)	36 (7.7)	2 (4.55)	
Skin	23 (4.48)	21 (4.5)	2 (4.55)	
Multiple	22 (4.29)	19 (4)	3 (6.82)	
Male reproductive	3 (0.58)	3 (0.64)	0	
Other (blood, synovial)	2 (0.39)	2 (0.43)	0	
Cancer treatments	387 (72.9)	366 (78)	21 (47.7)	
None	126 (24.56)	103 (22)	23 (52.27)	
Chemotherapy	136 (26.51)	132 (28)	4 (9.09)	
Radiation	36 (7)	33 (7)	3 (6.82)	
Chemotherapy + radiation	201 (38.2)	187 (39.87)	14 (31.82)	
Radiation to chest	93 (18.13)	83 (17.7)	10 (22.73)	<0.001
Immunotherapy (interferon; IL-2; G-CSF)	5 (0.97)	5 (1.1)	0	
Chemotherapy + immunotherapy	1 (0.19)	1 (0.21)	0	
Radiation + immunotherapy	5 (0.97)	5 (1.1)	0	
Chemotherapy + radiation + immunotherapy	3 (0.58)	3 (0.64)	0	
Time interval between final cancer therapy and index PET, yrs	1.8 (1–3.5)	1.8 (1–3.4)	2 (0.61–5)	0.67
Time interval between final cancer therapy and CVD event, yrs	5.2 (2.3–7.4)	n/a	5.20 (2.3–7.4)	n/a

Values are median (IQR), n (%), or mean ± SD. p Values are for the comparisons between participants with and without subsequent CVD. *Number of participants with available data on FRS = 260, CAC = 448, body mass index = 508 for the full cohort; CAC = 414 for the subgroup without CVD; CAC = 34 for the subgroup with CVD.
ATP III = Adult Treatment Panel III; CAC = coronary artery calcium; CVD = cardiovascular disease; FDG = fluorodeoxyglucose; FRS = Framingham risk score; G-CSF = granulocyte colony-stimulating factor; IL-2 = interleukin 2; IQR = interquartile range; n/a = not applicable; PET = positron emission tomography; TBR = target-to-background ratio.

Risk discrimination. With the data from the subgroup with complete data available for calculation of FRS (N = 260 individuals), the addition of FDG uptake to FRS scores modeled as continuous variables improved risk discrimination (concordance probability estimate or C-statistic [standard error]) over 6.5 years of follow-up: 0.66 (0.03) versus 0.62 (0.03). Further, incorporation of TBR into the model with FRS variables resulted in an integrated discrimination improvement of 5%. NRIs were 27.48% and 22.3% for the 10% and 6% intermediate-risk cut points for TBR measures (Tables 2 and 3), respectively. A sensitivity analysis evaluating uncorrected FDG uptake demonstrated that SUV_{max} also improved reclassification (although not as well as TBR), whereas SUV_{mean} was ineffective (Online Table S5).

DISCUSSION

Our investigations yielded several important observations. First, we demonstrated a significant association between aortic FDG uptake and incident CVD. Second, we observed that the addition of arterial FDG measures to traditional risk factors improved discrimination of subsequent CVD risk. Third, we observed that increasing arterial FDG-PET signals are inversely associated with the timing of CVD. Taken together, we demonstrated that the FDG-PET/CT signal measured within the
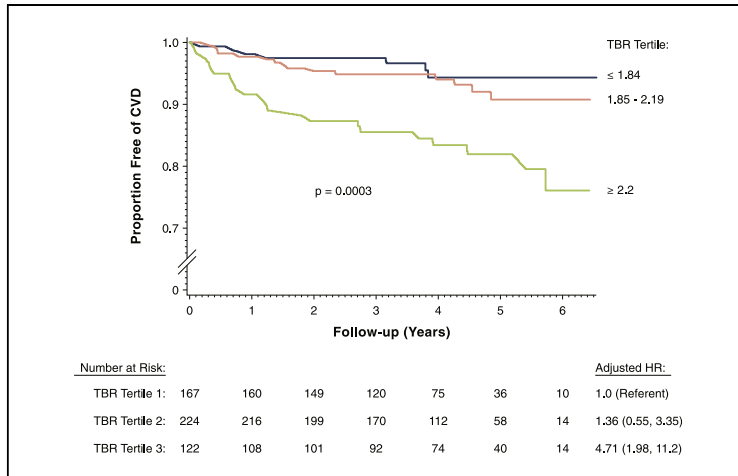
Figure 3. Proportion Free of CVD Stratified by TBR Tertiles

The p values from Kaplan-Meier survival curves were derived from log-rank test. Hazard ratios were derived from Cox proportional hazards regression. Values were adjusted for age, current smoking, hypertension, and hyperlipidemia, variables that showed significant association with CVD on univariate analysis from among established CV risk factors (age, sex, hypertension, diabetes, current smoking, and hyperlipidemia) and body mass index. The TBR was categorized based on the tertile distribution of the full cohort. HR = hazard ratio; other abbreviations as in Figures 1 and 2.

arterial wall provides added information that is useful for evaluating CVD risk in individuals who are undergoing routine FDG-PET/CT scans for oncological evaluation.

This arterial signal likely represents inflammatory activity within the artery wall. FDG uptake reflects the rate of glycolysis, which is particularly increased in activated proinflammatory macrophages (24,25) and FDG avidly accumulates as a
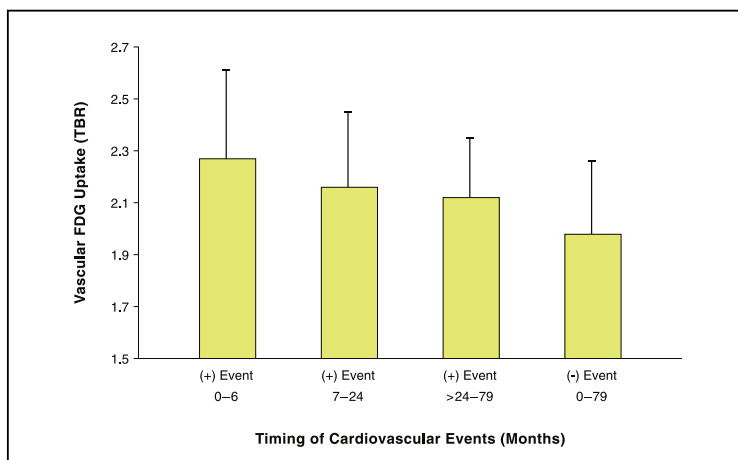
Figure 4. Association Between Vascular Inflammation and Timing of CV Events

The bar graphs show the average TBR (SD) in each of the groups of individuals who developed CVD at 0 to 6 months, 7 to 24 months, and >24 to 79 months and no events in 79 months, respectively. On linear regression analysis, aortic FDG uptake (TBR) was inversely related to the time interval between PET imaging and subsequent CVD, beta coefficient was −0.096 (p < 0.0001). Error bars represent SD. Abbreviations as in Figures 1 and 2.

result (26,27). FDG accumulation in the arterial wall localizes to macrophage-rich regions and correlates with immunohistochemical staining and gene expression for macrophage-specific markers (9,16,28), as well as circulating markers of inflammation (13,29). Further, arterial FDG uptake increases in proportion to atherosclerotic risk factors (30,31), with plaque morphological complexity (32), and after atherothrombotic events (8,33,34). Further, several studies have demonstrated that arterial FDG uptake is reduced by statins (35) and by drugs that are thought to inhibit inflammatory pathways (17,18).

The information provided by the PET/CT signal may be distinct from that provided by circulating biomarkers of inflammation. In this study, the observed adjusted risk (beyond FRS) for persons in the highest (vs. lowest) TBR tertile was approximately 3-fold greater compared with what has been historically observed for the inflammatory blood biomarker, high-sensitivity C-reactive protein (hs-CRP) (3). Further, the PET/CT signal provided a substantially higher NRI (22% to 27%) than that reported for hs-CRP (5.6% in the Framingham Heart Study [3] and 5.7% in the Women's Health Study [5]) or other blood biomarkers (6,7). It is possible that imaging (vs. blood) biomarkers provide additional prognostic information that is more relevant to the artery wall per se, whereas currently used blood biomarkers carry information from vascular as well as nonvascular sources.

Furthermore, PET/CT-measured arterial inflammation strongly predicted and significantly improved CVD risk discrimination beyond traditional risk factors (FRS). Additionally, our results demonstrated that the link between the PET signal and CVD was independent of the effects of CAC score on both the CVD outcomes and arterial inflammation. However, it is important to note that the CAC measurements in this study were derived from attenuation-correction computed tomography (ACCT) scans. Although CAC measurements obtained from ACCT scans have been shown to correlate well with those derived from dedicated CAC scans, the sensitivity for detection of low calcium values from nongated CT scans is reduced. Accordingly, the data from this study regarding the interrelationship between CAC score and PET imaging signal as they pertain to CVD risk should be interpreted cautiously.

The current study has several strengths. First, we blindly analyzed images that were obtained during routine PET/CT imaging, yet excluded only 2% of images (11 of 527) due to inadequacy of image quality, thus demonstrating that the majority of

routinely derived PET/CT examinations are of sufficient quality to produce this measure of CVD risk. Further, by including all consecutive patients that met our pre-specified criteria, this study provided a representative sample of cancer-free patients undergoing cancer surveillance and supports the generalizability of these findings to this population.

Additionally, the current study extends the findings of Rominger et al. (10) in 2 important ways. Although Rominger et al. (10) showed that the PET signal was associated with subsequent vascular events in a population of patients with active cancer, we demonstrated that: 1) FDG uptake, measured using PET/CT, strongly predicted subsequent CVD independently of traditional risk factors; and 2) this observation extended to individuals who were not receiving cancer chemotherapy. Furthermore, we demonstrated that the signal can be derived by measuring the aorta alone (as compared with measuring both the aorta and carotids, which is technically more challenging). Moreover, we showed that the arterial imaging data provide an opportunity to reclassify patient risk for CV events.

Study limitations. Several limitations primarily associated with the retrospective nature of the study should be noted. First, the fact that the study's sample population was drawn from a clinical database (the majority of whom are cancer survivors) limits the generalizability of these findings beyond that population. Further, given that the patients who were studied were not prospectively recruited, there is a limited opportunity to compare the imaging findings with additional blood biomarkers that are related to CV risk (such as CRP). Additionally, the data used to adjudicate events were limited to that contained within the medical record; hence, some events might have been missed or misclassified. Nonetheless, it is anticipated that this would lead to an overall underestimation of the technique's prognostic value. Furthermore, the use of clinically derived PET and CT images does not take advantage of methods that have been used to optimize the arterial FDG signal. Notably, image acquisition at 1 h after tracer injection (which is typically done for routine clinical examinations) may be rather early for arterial wall imaging because some (8,15) but not all (36) prior studies have suggested an enhanced ability to measure arterial wall activity at 3 (vs. 1) h after FDG injection.

Taken together, the results of the present study underscore the potential clinical utility of FDG-PET measurement of arterial activity to enhance the delineation of CVD risk in individuals undergoing oncological evaluation and surveillance, particularly cancer survivors. In this population, FDG-PET imaging is routinely performed; thus, it may be reasonable to take advantage of the readily available information to help guide clinicians in their preventive and management strategies without the need to add imaging costs or burden of additional radiation exposure. Furthermore, the subpopulation of cancer survivors has grown substantially over the years (37) and CVD has become a leading cause of morbidity and mortality in this subpopulation (38,39). Accordingly, the derivation of risk stratification data from routine PET/CT images may be of considerable utility in this group.

Additionally, the present result further supports the use of PET/CT imaging to evaluate the efficacy of novel therapies that target atherosclerotic inflammation (19,40). However, further validation is needed to assess whether this imaging approach is

Table 2. Summary of Net Reclassification Among Patients With Complete Framingham Risk Variables

Risk Categories	NRI (95% Bootstrap CI) (FRS + TBR)	Proportion (Events) Correctly Reclassified	Proportion (Nonevents) Correctly Reclassified
<10%; 10%–20%; >20%	27.48% (16.27–39.92)	12.66%	14.82%
<6%; 6%–20%; >20%	22.3% (11.54–35.42)	12.31%	9.99%

TBR was modeled as continuous variable.
CI = confidence interval; NRI = net reclassification improvement; other abbreviations as in Table 1.

Table 3. Reclassification of Patients Without CVD at Index FDG-PET Who Did and Did Not Develop CVD

Framingham Risk Variables* (Model A)	Framingham Risk Variables + FDG Uptake (TBR) (Model B)			
	<10% risk n (%)	10%–20% risk n (%)	>20% risk n (%)	Total
Participants with subsequent CVD				
<10% risk	3	0	0	3
10%–20% risk	0	2 (25.00)	6 (75.00)	8
>20% risk	0	0	29 (100.00)	29
Total	3	2	35	40
Participants without subsequent CVD				
<10% risk	103 (96.26)	3 (2.80)	1 (0.93)	107
10%–20% risk	29 (50.00)	19 (32.76)	10 (17.24)	58
>20% risk	1 (1.82)	15 (27.27)	39 (70.91)	55
Total	133	37	50	220

*Framingham risk variables included age (continuous), male or female sex (binary), current smoking (binary), presence or absence of diabetes (binary), total cholesterol (continuous), high-density lipoprotein (continuous), systolic blood pressure (continuous), and antihypertensive therapy (binary); TBR was modeled as a continuous variable.
Abbreviations as in Table 1.

sufficiently valuable to outweigh the associated cost (Medicare reimbursement rate of approximately $1,160) and risks (such as radiation exposure of up to 7 mSv) in other groups of patients who would not otherwise undergo PET/CT imaging for pre-existing clinical indications.

CONCLUSIONS

FDG-PET–measured arterial inflammation substantially improved CVD event prediction and risk stratification beyond FRS in a population of cancer-free participants undergoing cancer surveillance without prior history of clinical CVD. These data also suggest that routinely derived PET/CT images contain data that could be mined to improve the CV risk stratification of cancer survivors, and after further study, may prove useful in additional populations.

Reprint requests and correspondence: Dr. Ahmed Tawakol, Massachusetts General Hospital, 165 Cambridge Street, Suite 400, Boston, Massachusetts 02114-2750. *E-mail:* *atawakol@partners.org.*

REFERENCES

1. Third Report of the National Cholesterol Education Program (NCEP) Expert Panel on Detection, Evaluation, and Treatment of High Blood Cholesterol in Adults (Adult Treatment Panel III) final report. Circulation 2002;106:3143–421.

2. Wilson PW, D'Agostino RB, Levy D, Belanger AM, Silbershatz H, Kannel WB. Prediction of coronary heart disease using risk factor categories. Circulation 1998;97:1837–47.

3. Wilson PW, Pencina M, Jacques P, Selhub J, D'Agostino R Sr, O'Donnell CJ. C-reactive protein and reclassification of cardiovascular risk in the Framingham Heart Study. Circ Cardiovasc Qual Outcomes 2008;1:92–7.

4. Shah T, Casas JP, Cooper JA, et al. Critical appraisal of CRP measurement for the prediction of coronary heart disease events: new data and systematic review of 31 prospective cohorts. Int J Epidemiol 2009;38:217–31.

5. Ridker PM, Buring JE, Rifai N, Cook NR. Development and validation of improved algorithms for the assessment of global cardiovascular risk in women: the Reynolds risk score. JAMA 2007;297:611–9.

6. Di Angelantonio E, Gao P, Pennells L, et al. Lipid-related markers and cardiovascular disease prediction. JAMA 2012;307:2499–506.

7. Melander O, Newton-Cheh C, Almgren P, et al. Novel and conventional biomarkers for prediction of incident cardiovascular events in the community. JAMA 2009;302:49–57.

8. Rudd JH, Warburton EA, Fryer TD, et al. Imaging atherosclerotic plaque inflammation with ^{18}F-fluorodeoxy-glucose positron emission tomography. Circulation 2002;105:2708–11.

9. Tawakol A, Migrino RQ, Bashian GG, et al. In vivo ^{18}F-fluorodeoxyglucose positron emission tomography imaging provides a noninvasive measure of carotid plaque inflammation in patients. J Am Coll Cardiol 2006;48:1818–24.

10. Rominger A, Saam T, Wolpers S, et al. ^{18}F-FDG PET/CT identifies patients at risk for future vascular events in an otherwise asymptomatic cohort with neoplastic disease. J Nucl Med 2009;50:1611–20.

11. Paulmier B, Duet M, Khayat R, et al. Arterial wall uptake of fluorodeoxyglucose on PET imaging in stable cancer disease patients indicates higher risk for cardiovascular events. J Nucl Cardiol 2008;15:209–17.

12. D'Agostino RB Sr, Vasan RS, Pencina MJ, et al. General cardiovascular risk profile for use in primary care: the Framingham Heart Study. Circulation 2008;117:743–53.

13. Subramanian S, Tawakol A, Burdo TH, et al. Arterial inflammation in patients with HIV. JAMA 2012;308:379–86.

14. Rudd JH, Myers KS, Bansilal S, et al. [18]Fluorodeoxyglucose positron emission tomography imaging of atherosclerotic plaque inflammation is highly reproducible: implications for atherosclerosis therapy trials. J Am Coll Cardiol 2007;50:892–6.

15. Rudd JH, Myers KS, Bansilal S, et al. Atherosclerosis inflammation imaging with ^{18}F-FDG PET: carotid, iliac, and femoral uptake reproducibility, quantification methods, and recommendations. J Nucl Med 2008;49:871–8.

16. Font MA, Fernandez A, Carvajal A, et al. Imaging of early inflammation in low-to-moderate carotid stenosis by 18-FDG-PET. Front Biosci 2009;14:3352–60.

17. Mizoguchi M, Tahara N, Tahara A, et al. Pioglitazone attenuates atherosclerotic plaque inflammation in patients with impaired glucose tolerance or diabetes a prospective, randomized, comparator-controlled study using serial FDG PET/CT imaging study of carotid artery and ascending aorta. J Am Coll Cardiol Img 2011;4:1110–8.

18. Elkhawad M, Rudd JH, Sarov-Blat L, et al. Effects of p38 mitogen-activated protein kinase inhibition on vascular and systemic inflammation in patients with atherosclerosis. J Am Coll Cardiol Img 2012;5:911–22.

19. Fayad ZA, Mani V, Woodward M, et al. Safety and efficacy of dalcetrapib on atherosclerotic disease using novel non-invasive multimodality imaging (dal-PLAQUE): a randomised clinical trial. Lancet 2011;378:1547–59.

20. Blaha MJ, Budoff MJ, DeFilippis AP, et al. Associations between C-reactive protein, coronary artery calcium, and cardiovascular events: implications for the JUPITER population from MESA, a population-based cohort study. Lancet 2011;378:684–92.

21. Gonen M. Analyzing Receiver Operating Characteristic Curves With SAS. Cary, NC: SAS Institute Inc., 2007.

22. Pencina MJ, D'Agostino RB Sr., Steyerberg EW. Extensions of net reclassification improvement calculations to measure usefulness of new biomarkers. Stat Med 2011;30:11–21.

23. Shaw LJ, Raggi P, Schisterman E, Berman DS, Callister TQ. Prognostic value of cardiac risk factors and coronary artery calcium screening for all-cause mortality. Radiology 2003;228:826–33.

24. Garedew A, Henderson SO, Moncada S. Activated macrophages utilize glycolytic ATP to maintain mitochondrial membrane potential and prevent apoptotic cell death. Cell Death Differ 2010;17:1540–50.

25. Cramer T, Yamanishi Y, Clausen BE, et al. HIF-1alpha is essential for myeloid cell-mediated inflammation. Cell 2003;112:645–57.

26. Kubota R, Kubota K, Yamada S, Tada M, Ido T, Tamahashi N. Microautoradiographic study for the differentiation of intratumoral

macrophages, granulation tissues and cancer cells by the dynamics of fluorine-18-fluorodeoxyglucose uptake. J Nucl Med 1994;35:104–12.

27. Satomi T, Ogawa M, Mori I, et al. Comparison of contrast agents for atherosclerosis imaging using cultured macrophages: FDG versus ultrasmall superparamagnetic iron oxide. J Nucl Med 2013;54:999–1004.

28. Graebe M, Pedersen SF, Borgwardt L, Hojgaard L, Sillesen H, Kjaer A. Molecular pathology in vulnerable carotid plaques: correlation with [18]-fluorodeoxyglucose positron emission tomography (FDG-PET). Eur J Vasc Endovasc Surg 2009;37:714–21.

29. Choi HY, Kim S, Yang SJ, et al. Association of adiponectin, resistin, and vascular inflammation: analysis with ^{18}F-fluorodeoxyglucose positron emission tomography. Arterioscler Thromb Vasc Biol 2011;31:944–9.

30. Tahara N, Kai H, Yamagishi S, et al. Vascular inflammation evaluated by ^{18}F-fluorodeoxyglucose positron emission tomography is associated with the metabolic syndrome. J Am Coll Cardiol 2007;49:1533–9.

31. Rudd JH, Myers KS, Bansilal S, et al. Relationships among regional arterial inflammation, calcification, risk factors, and biomarkers: a prospective fluorodeoxyglucose positron-emission tomography/computed tomography imaging study. Circ Cardiovasc Imaging 2009;2:107–15.

32. Figueroa AL, Subramanian SS, Cury RC, et al. Distribution of inflammation within carotid atherosclerotic plaques with high-risk morphological features: a comparison between positron emission tomography activity, plaque morphology, and histopathology. Circ Cardiovasc Imaging 2012;5:69–77.

33. Rogers IS, Nasir K, Figueroa AL, et al. Feasibility of FDG imaging of the coronary arteries: comparison between acute coronary syndrome and stable angina. J Am Coll Cardiol Img 2010;3:388–97.

34. Davies JR, Rudd JH, Fryer TD, et al. Identification of culprit lesions after transient ischemic attack by combined ^{18}F fluorodeoxyglucose positron-emission tomography and high-resolution magnetic resonance imaging. Stroke 2005;36:2642–7.

35. Tahara N, Kai H, Ishibashi M, et al. Simvastatin attenuates plaque inflammation: evaluation by fluorodeoxyglucose positron emission tomography. J Am Coll Cardiol 2006;48:1825–31.

36. Menezes LJ, Kotze CW, Hutton BF, et al. Vascular inflammation imaging with ^{18}F-FDG PET/CT: when to image? J Nucl Med 2009;50:854–7.

37. Jemal A, Siegel R, Xu J, Ward E. Cancer statistics, 2010. CA Cancer J Clin 2010;60:277–300.

38. Carver JR, Ng A, Meadows AT, Vaughn DJ. Cardiovascular late effects and the ongoing care of adult cancer survivors. Dis Manag 2008;11:1–6.

39. Hooning MJ, Botma A, Aleman BM, et al. Long-term risk of cardiovascular disease in 10-year survivors of breast cancer. J Natl Cancer Inst 2007;99:365–75.

40. Tawakol A, Fayad ZA, Mogg R, et al. Intensification of statin therapy results in a rapid reduction in atherosclerotic inflammation: results of a multi-center FDG-PET/CT feasibility study. J Am Coll Cardiol 2013;62:909–17.

Key Words: cardiovascular events ■ FDG-PET ■ inflammation ■ risk factors.

▶ **APPENDIX**

For supplemental material, please see the online version of this article.